Predictive speed control of induction drive with high-frequency torsional oscillation

Piotr J. Serkies, Krzysztof Szabat, Mateusz Dybkowski
Wroclaw University of Technology
50-372 Wrocław, ul. Smoluchowskiego 19, e-mail: {piotr.serkies, krzysztof.szabat, mateusz.dybkowski}@ pwr.wroc.pl

In the paper issues related to the use of model predictive control (MPC) of the drive system with an elastic coupling and an induction motor are presented. After a short introduction the mathematical model of the driving motor with a vector control structure and the two-mass drive system are described. Then, the idea of the MPC is introduced. Next the exact formulation of the MPC for a two-mass drive system is shown. In the MPC algorithm the constraints of the inner and control variables are taken into consideration. The results obtained in the simulation study confirm the correct work of the investigated structure.

1. Introduction

A demand for the minimalization and reducing the total moment of inertia which allows to shorten the response time of the whole system is evident in modern drives system. However, reducing the size of the mechanical elements may result in disclosure of the finite stiffness of the drive shaft, which can lead to the occurrence of torsional vibrations. This problem is common in rolling-mill drives, belt-conveyors, paper machines, robotic-arm drives including space manipulators, servo-drives and throttle systems [1] – [10].

Many control structures have been proposed for the torsional vibrations damping of the two-mass drive system [1] – [12]. The most popular approach relies on the application of additional feedback(s) from selected state variable(s) [1] – [2]. Those structures are effective in the case of the system with known and constant parameters. A drive system with changeable (or unknown) parameters requires more sophisticated control paradigms such as non-linear or adaptive control. Sliding mode based structures are proposed in [4] – [9], to achieve good level of robustness to plant parameter variations. Examples of the adaptive control structure are shown in [10] – [11].

In the recent years, model predictive control (MPC) has been widely investigated for its potential in controlling modern electrical drives and power electronics circuits [12] – [14]. Predictive control presents several advantages that make it suitable for the control of power converters and drives. The central feature of MPC is that it enables the process operating and physical constraints (due to e.g.

resource limitations, operational or safety concerns as well as limits arising from various economic objectives) to be taken directly into consideration in the control problem formulation so that any potential constraint violations are anticipated and prevented. Additionally, as the control input is obtained by solving an optimization problem at each sampling time, it can ensure truly optimal performance of the closed-loop control system.

The main goal of this paper is to present and discuss simulation results related to the MPC of a two-mass system. Contrary to some previous works [13], [14], the DC driving machine has been replaced in this work with an induction motor. Although the mechanical part of the drive system remains the same, the change of the torque control loop from the simple one (DC motor) to very complicated (field-oriented controlled induction motor) can influence the properties of the whole control structure. Additionally, the frequency of torsional oscillations is more than ten times higher than in [13]. The main goal of the paper is to investigate how these two factors influence the system performance.

2. The induction motor drive with field oriented control structure

Induction motors (IM) are used more and more widely in different industrial installations. IM are durable, they do not need much servicing and are relatively cheap, yet they are nonlinear objects and thus require advanced control methods. The direct field-oriented control structure (DFOC), presented in Fig. 1, is recently commonly used IM control scheme. It needs information about the rotor flux vector magnitude and position to perform precise direct flux control and the transformation from *a-b-c* to *x-y* as well as α-β reference frames and vice versa. Field-oriented control [16] makes it possible to separate control of the rotor flux – by means of the stator current vector component i_{sx} and electromagnetic torque control – by means of the second current component i_{sy}. It utilises a similar torque control method as in the separately excited DC machine. The rotor flux vector of IM has to be calculated on the basis of suitable estimator [16] using measured stator currents and voltages as well as IM parameters. Errors in all those factors influence the computed value of the rotor flux vector and thus accuracy of the whole torque control loop in a negative way. They can also reduce the performance of the outer (speed) loop.

Usually the external speed controller for two-mass system with additional feedbacks is designed with the assumption, that the internal torque control loop is very fast and reacts without any delay [2]. In the case of the DFOC induction motor drive the internal torque control loop contains relatively complicated structure, which can cause some delay (and nonlinearities) in the torque control (in comparison with very simple DC drive case). Thus the effectiveness of the external MPC speed controller, designed in the same way as for linear system without internal delay, is tested based on the estimated state variables.

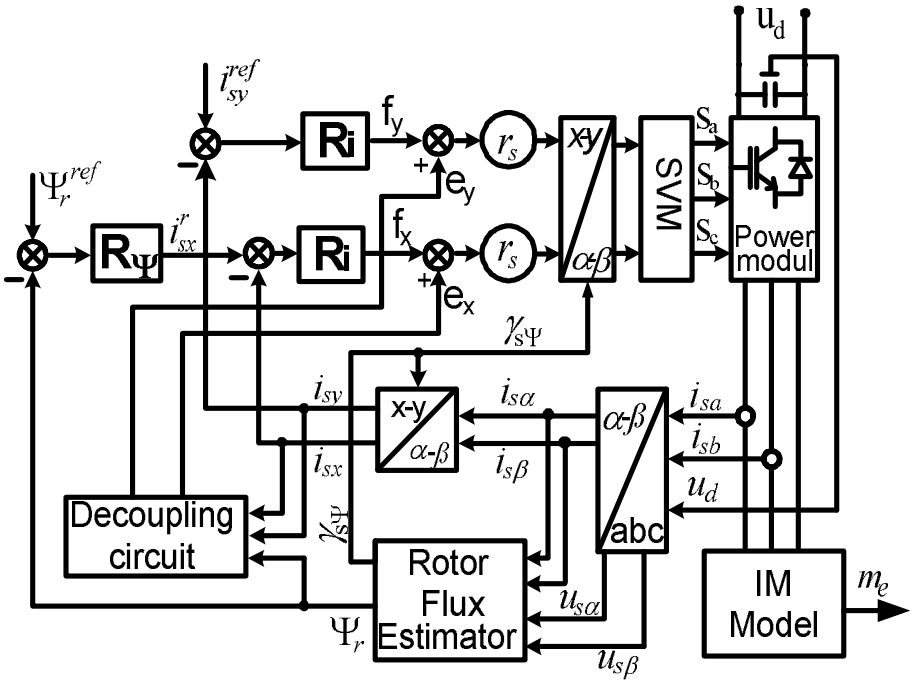

Fig. 1. The block diagram of DFOC

3. Two-mass drive system

Many industrial drive systems can be modelled as two-mass systems, where the first mass represents the moment of inertia of the motor and the second mass refers to the moment of inertia of the load machine. In this paper, the commonly used inertia-free-shaft dual-mass system model will be employed, which is described by the following normalized differential equations [2]:

$$T_1 \frac{d\omega_1(t)}{dt} = m_e(t) - m_s(t) \tag{1}$$

$$T_2 \frac{d\omega_2(t)}{dt} = m_s(t) - m_L(t) \tag{2}$$

$$T_c \frac{dm_s(t)}{dt} = \omega_1(t) - \omega_2(t) \tag{3}$$

where: ω_1 ,ω_2 – motor and load speeds, m_e, m_s, m_L – electromagnetic, shaft ad load torques, T_1, T_2 – mechanical time constant of the motor and the load machine, T_c – stiffness time constant and T_α – position time constant.

The schematic diagram of a dual-mass system is shown in Fig. 2.

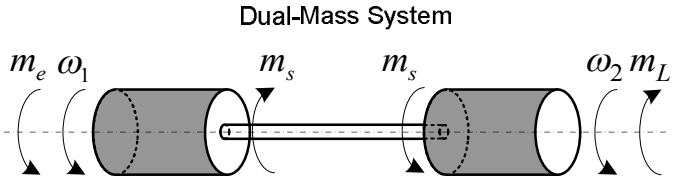

Fig. 2. The ideal diagram of the two-mass system

In most cases, the internal damping coefficient d is very small and can be neglected in the synthesis of the control system.

The resonant f_r and antiresonant f_{ar} frequencies of the two-mass system are defined as follows:

$$f_r = \frac{1}{2\pi}\sqrt{K_c \frac{J_1 + J_2}{J_1 J_2}}, \qquad f_{ar} = \frac{1}{2\pi}\sqrt{\frac{K_c}{J_2}} \tag{4}$$

The value of the resonant frequency depends on the type of the drive and can vary from a few hertz in a paper machine section [17], through dozens of hertz in a rolling-mill drive [18], and can exceed hundreds hertz in a modern servo-drives [14]. The value of the antiresonant frequency can be even ten times smaller than the resonant one in a dryer [2], but usually the difference is much smaller (smaller than two).

The next parameter commonly provided for analysis of the two-mass system is inertia ratio defined as:

$$R = \frac{J_2}{J_1} = \frac{T_2}{T_1} \tag{5}$$

4. MPC-based control structure

In model predictive control, an explicit model of the plant is used to predict the effect of future actions of the manipulated variables on the process output. The performance of the system (whether predicted or actual) will be assessed through a cost function [19], [20]:

$$J = \sum_{k=0}^{\infty} y_k^T Q y_k + u_k^T R u_k \tag{6}$$

where $Q \geq 0$ and $R > 0$ are the weighting matrices. In (6), y_k denotes the value of the output vector at a future time k, given an input sequence u_k, an initial state x_0 of the system. At each time step k an MPC algorithm attempts to optimize future plant behavior while respecting the system input/output constraints by computing a sequence of control actions.

The MPC algorithm based on problem (6) can be implemented in two ways. The traditional approach relies on solving the optimization problem on-line for a given *x(k)* in a receding-horizon fashion. This means that, at the current time *k*, only the first element control signal u_k of the optimal input sequence is actually implemented to the plant and the rest of the control moves u_{k+1} are discarded. At the next time step, the whole procedure is repeated for the new measured or estimated state *x(k+1)* [20]. This strategy can be computationally demanding for systems requiring fast sampling or low-performance computers and hence greatly restricting the scope of applicability to systems with relatively slow dynamics. In the second approach, the problem (6) is first solved off-line for all state realizations $x \in X_f$ with the use of multi-parametric programming [20]. Specifically, by treating the state vector *x(k)* as a parameter vector, it can be shown that the parameter space X_f can be subdivided into characteristic regions, where the optimizer is given as an explicit function of the parameters. This profile is a piecewise affine state feedback law:

$$U(x) = K_r x + g_r, \qquad \forall x \in P_r \tag{7}$$

where P_r are polyhedral sets defined as:

$$P_r = \left\{ x \in \Re^n \mid H_r x \le d_r \right\}, \qquad r = 1,...N_r \tag{8}$$

Algorithms for the construction of a polyhedral partition of the state space and computation of a PWA control law are given in [20] – [24]. In its simplest form, the PWA control law (7) – (8) can be evaluated by searching for a region containing current state *x* in its interior and applying the affine control law associated with this region. More efficient search strategies which offer a logarithmic-type complexity with respect to the total number of regions Nr in the partition have also been developed. Nonetheless, the implementation of the explicit MPC control law can often be several orders of magnitude more efficient than solving the optimization problem (6) directly. This gain in efficiency is crucial for demanding applications with fast dynamics or high sampling rates in the milli/micro second range, such as the drive system considered in this paper. A more exact description of the MPC strategy and its explicit solution is presented [20] – [24].

The block diagram of the considered control structure presented in Fig. 3.

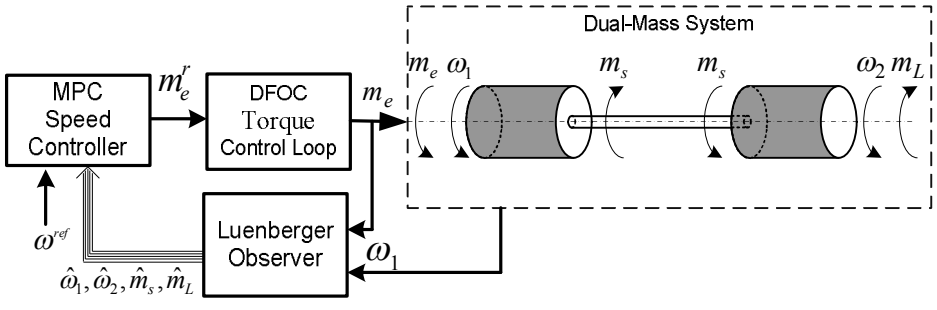

Fig. 3. The block diagram of the analysed control structure with MPC speed controller

It consists of the following blocks:
- a dual-mass system,
- a DFOC torque control loop,
- a predictive speed controller,
- a Luenberger observer used for estimation of the system state variables (it is assumed that only the motor torque and the motor speed are available for control purposes).

The original state vector of the two-mass drive system has been extended by three additional variables which describ the dynamic of the load torque, reference value and the electromagentic torque. The dynamics of the two variables mentioned firstly is unknown so it is assumed:

$$\frac{d}{dt}m_L = 0 \tag{9}$$

$$\frac{d}{dt}\omega^{ref} = 0 \tag{10}$$

The dynamics of the electromagnetic torque transients is described by the following equations:

$$\frac{d}{dt}m_e = -\frac{1}{T_{me}}m_e^r \tag{11}$$

Taking into account the abovementioned variables, the analyzed state vector has the following form:

$$X_c = \left[m_e \quad \omega_1 \quad \omega_2 \quad m_s \quad m_L \quad \omega^{ref}\right]^T \tag{12}$$

The model described by eq. (1), (9) – (11) has been transformed to a discrete model with sampling time T_s. The following constraints are imposed for all k:

$$\begin{aligned} -3 \le m_e \le 3 \\ -1.5 \le m_s \le 1.5 \end{aligned} \tag{13}$$

The vector y used in (6) has the following form:

$$\begin{aligned} y_1 &= \omega_1 - \omega^{ref}, \\ y_2 &= \omega_2 - \omega^{ref}, \\ y_3 &= m_s - m_L, \\ y_4 &= \omega_1 - \omega_2. \end{aligned} \tag{14}$$

The first and the second terms of (14) minimize the difference between the motor and load speed and the reference value while the third term minimizes the difference between the shaft and the load torque and the last term calculates the difference between the two speeds.

The resulting formulation of (6) can be given in the following form:

$$\min_{u_1,u_2,\cdots,u_{Nc-1}} \sum_{k=0}^{N} q_1(y_1(k))^2 + q_2(y_2(k))^2 + q_3(y_3(k))^2 + q_4(y_4(k))^2 + \\ + \sum_{j=1}^{Nc-1} r\left(m_e^r(j)\right)^2 \tag{15}$$

where: $q_1 \ldots q_4$ – weights for the victor y, r – weight for control signal, N – length of the horizon window, N_c – control horizon.

5. Results

In order to validate the feasibility and effectiveness of the proposed approach, a comprehensive simulation study has been carried out. In this synopsis, only a number of selected transients are presented. The study has been done with the help of the Matlab-Simulink simulation packet. The used model has different sampling times. The fastest sampling period has the induction motor and the two mass system model – *2 μs*. The observer has been calculated with the period 100 *μs*; and the predictive controller with 500 *μs*.

The parameters of the mechanical part of the drive have been as follows: the stiffness time constant *Tc = 100 μs* and the mechanical time constant of the driving motor T_1 *= 100 ms*. The mechanical time constant of the load machine has been changing between 25 and 200 *ms*. As mentioned in the previous section, the maximal allowed value of the electromagnetic torque has been set to ±3, and for the shaft torque to ±1.5 of its nominal value. The frequency characteristic of the analyzed system for different value of *R* are shown in Fig. 4.

As can be concluded from Fig. 4, the resonant frequency of the systems exceed hundreds of Hertz, contrary to some previous works [13] – [14] where frequency of torsional vibration was much smaller.

First the correctness of the work of the DFOC control structure has been examined. In Fig. 5 the electromagnetic torque responses as well as the flux responses of the induction motor to the step changes of the reference torque are shown.

As can be concluded from the presented transients, the response time of the modulus of the rotor flux is about 10ms (Fig. 5b). Therefore, in the next study the induction motor is first excited (the flux is set to the nominal value) and then the drive is ready to work. Rapid changes of the electromagnetic torque have almost no influence on the transients of the flux. Transients of the electromagnetic torque under rapid changes of its reference value is shown in Fig. 5a. The torque follows its reference value without oscillations and with the setting time approximately *800μs* (for the step changes equal to the nominal value). So, the presented figures confirm the correct work of the DFOC control structure.

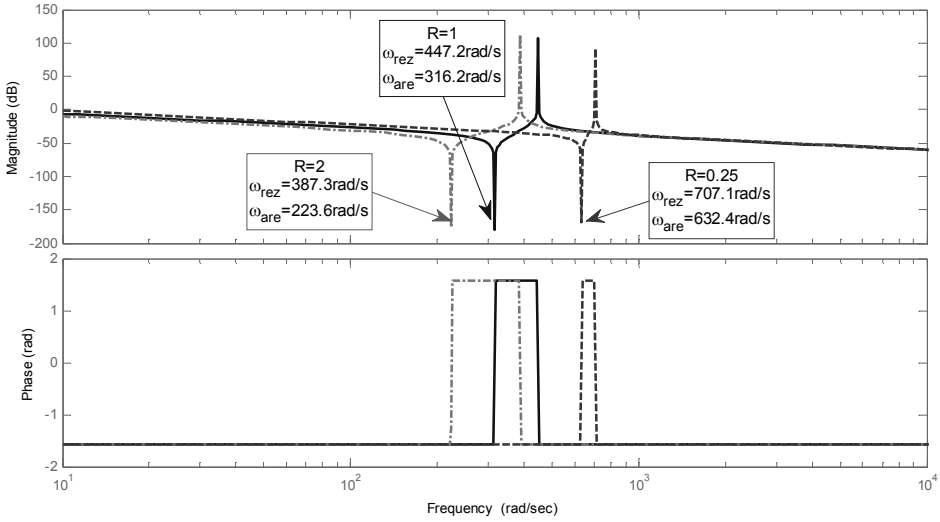

Fig. 4. Frequency characteristic of the analyzed systems

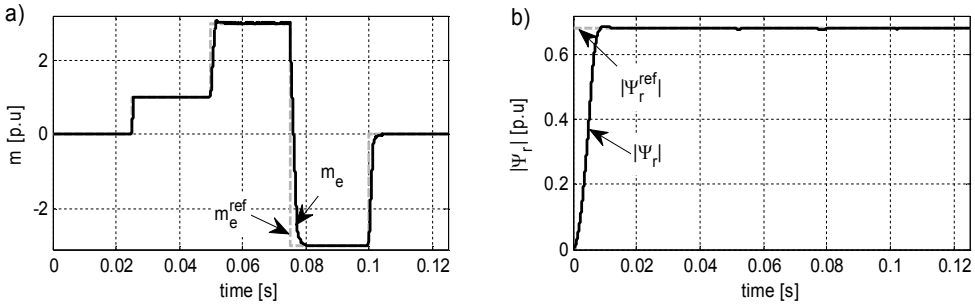

Fig. 5. Responses of the electromagnetic torque (a) , and the modulus of the rotor flux (b) in DFOC control structure to the step changes of the reference value

Then, the whole control structure including the DFOC scheme and the predictive speed controller working with the Luenberger observer has been investigated. The two-mass drive system with different inertia ratio R = 2 (ω_{rez} = 387.3rad/s), R = 1 (ω_{rez} = *447.2*/s), and R = 4 (ω_{rez} = *707.1*rad/s) has been tested. The parameters of the predictive control strategy used for the different inertia ratio are shown in Table 1.

Table 1. The utilized parameters of the MPC for different inertia ratio

	diag(Q)	r	N	N_c
R = 2	[10500 10500 8 1000]	2	10	2
R = 1	[550 550 8 1000]	2	10	2
R = 0.25	[430 430 80 10]	8	20	2

The explicit MPC controller has been computed using the Multi-Parametric Toolbox (MPT). In Fig. 6 two-dimensional cuts through the polyhedral partition corresponding to $[\omega_2, m_s]$ and $[m_e, \omega_1]$ are depicted for illustration.

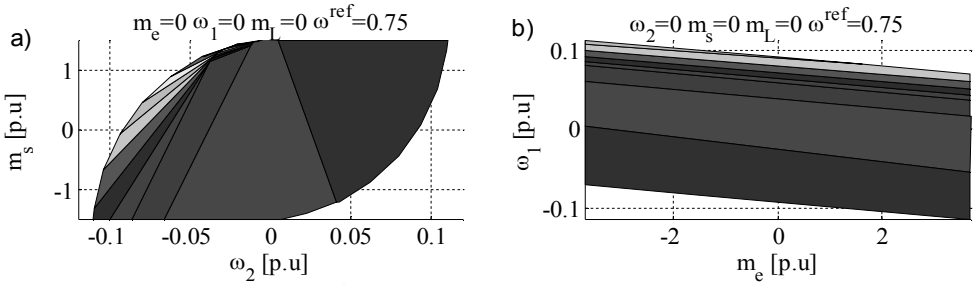

Fig. 6. Closed-loop partitions defined over $[m_s\ \omega_2]$ (a), $[\omega_1\ m_e]$ (b)

The tested system has the following operation scheme. At time t_1 = 0.05s the reference value of the speed is set to 0.75 of its nominal value. As can be seen in Fig. 7a, the electromagnetic torque response is very fast. It is clearly visible in the some figure that there are no validation in the shaft torque transient. The start-up takes approximately 0.16 s. The load torque is applied at the time t_2 = 0.2 s, which causes the small but visible disruption in the speeds transients. The transients of the i_{sx} and the i_{sy} in DFOC control structure is presented in Fig. 7c and the active controller region in Fig. 7d. The transients of the system with different inertia ratio R = 1 and R = 0.25 are presented in Fig. 8 and 9 respectively.

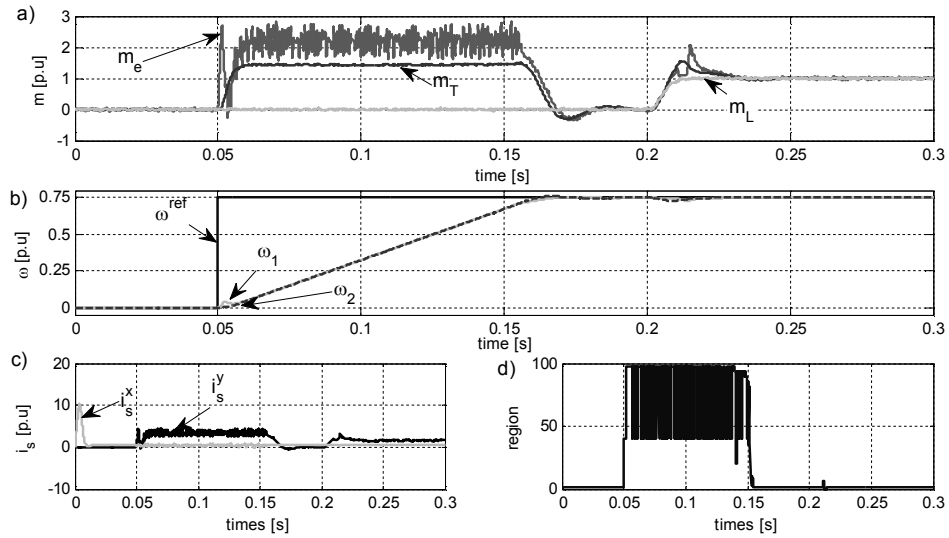

Fig. 7. Transients of the system for R = 2: a) torques, b) speeds, c) currents in axis x and y, d) actives regions

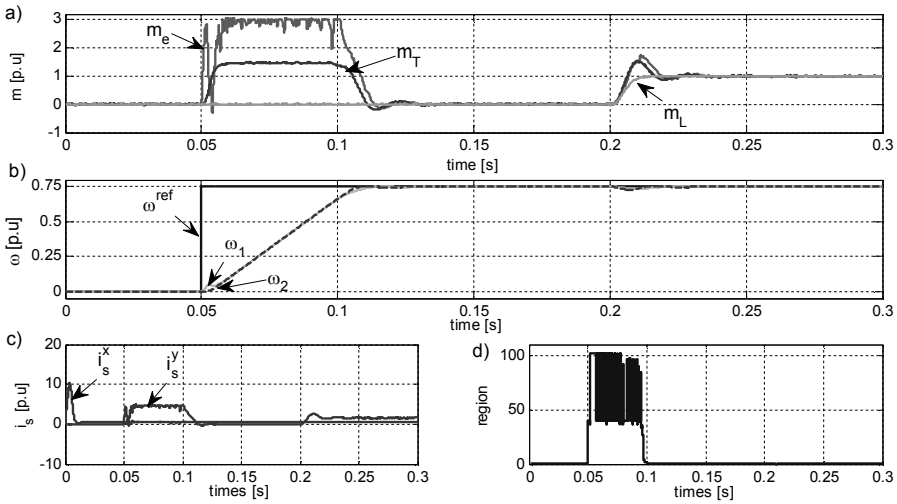

Fig. 8. Transients of the system for R = 1: a) torques, b) speeds, c) currents in axis x and y, d) actives regions

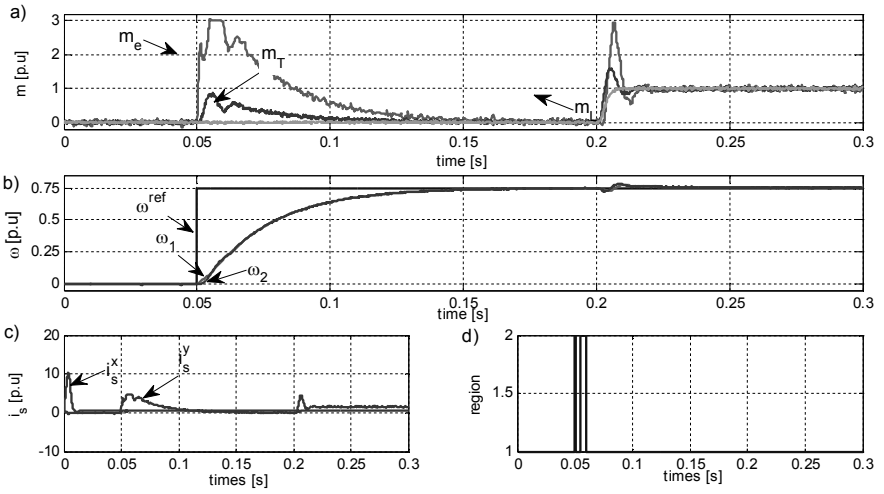

Fig. 9. Transients of the system for R = 0.25: a) torques, b) speeds, c) currents in axis x and y, d) actives regions

As can be concluded from presented transients the proposed control structure works in a correctly. The torsional vibrations are effectively damped in both examined systems. In the case of the big value of the inertia ratio (R = 2) the decrease of the system dynamic is visible. It comes from the fact that the total moment of inertia of such system is much bigger than the moment of inertia of the system with smaller value of the inertia ratio. The system can become faster by suitable increase the values of q_1 and q_2.

6. Conclusion

In the paper issues related to the application of the MPC control structure to the drive system with an induction motor and the two-mass system are presented. The DFOC control structure has been applied to control the electromagnetic torque. The predictive speed controller works with the Luenberger observer which is used to estimate the non-measurable state variables of the system.

As can be concluded from the presented results, the drive system works correctly for different configuration of the mechanical part of the drive. The sets of the control constraints related to the shaft torque and electromagnetic torque are not validated. It means that the control structure based on the MPC can ensure safe work in a drive system with elastic transmission. The replace of the simple electromagnetic torque control loop (DC motor) by the much more complicated one (DFOC) does not influence the properties of the drive.

The future work will be devoted to designing of an MPC control structure robust to parameter variation with respect to the shape of its transients. Also an experimental verification of the proposed solution is one of the main point of the future work.

References

[1] Orlowska-Kowalska T., Szabat K., Control of the Drive System with Stiff and Elastic Couplings Using Adaptive Neuro-Fuzzy Approach, IEEE Trans. on Industrial Electronics, vol. 54, no.1, pp. 228-240, 2007.

[2] Szabat K., Struktury sterowania elektrycznych układów napędowych z połączeniem sprężystym. Prace Naukowe Instytutu Maszyn, Napędów i Pomiarów Elektrycznych Politechniki Wrocławskiej nr 61, Wrocław 2008.

[3] Korondi P., H. Hashimoto H., Utkin V., Direct torsion control of flexible shaft in an observer-based discrete-time sliding mode, IEEE Trans. on Ind. Electronics, pp. 291-296, vol. 45, no.2, 1998.

[4] Szabat K., Orlowska-Kowalska T., Performance Improvement of Industrial Drives with Mechanical Elasticity Using Nonlinear Adaptive Kalman Filter, IEEE Trans. on Industrial Electronics, vol. 55, no. 3, pp. 1075-1084, 2008.

[5] Hace A., Jezernik K., Sabanovic A., Improved Design of VSS Controller for a Linear Belt-Driven Servomechanism, IEEE/ASME Trans. on Mechatronics, pp 385-390, vol. 10, no.4, 2005.

[6] Ryvkin S., Izosimov D., Bayda S., Flex mechanical digital control design, Proceedings of IEEE International Conference on Industrial Technology, IEEE ICIT'03, vol.1, 2003, pp. 298-302.

[9] Vittek J., Makys P., Stulrajter M., Dodds S.J., Perryman R., Comparison of sliding mode and forced dynamics control of electric drive with a flexible coupling employing PMSM, IEEE Int. Conf. on Industrial Technology ICIT 2008, 2008, on CD, China.

[10] Szabat, K., Orlowska-Kowalska T., "Performance Improvement of Industrial Drives with Mechanical Elasticity using Nonlinear Adaptive Kalman Filter", IEEE Trans. Industrial Electronics, vol.55, no. 3, 2008, pp.1075-1084.
[11] Hirovonen M., Pyrhonen O., Handroos H., "Adaptive nonlinear velocity controller for a flexible mechanism of a linear motor", Mechatronics, Elsevier, vol. 16, no. 5, 2006, pp.279-290.
[12] Cortés P., Kazmierkowski M.P., Kennel R.M., Quevedo D.E., Rodriguez J., Predictive control in power electronics and drives, IEEE Trans. Industrial Electronics, vol. 55, no. 12, pp. 4312–4324, Dec. 2008.
[13] Szabat K., Serkies P., Zastosowanie sterowania predykcyjnego w układzie napędowym z połączeniem sprężystym. Przegląd Elektrotechniczny vol. 86, no. 2, pp. 380–383, 2010.
[14] Szabat K., Serkies P., Nalepa R, Cychowski M., Predictive Position Control of Elastic Dual-Mass Drives under Torque and Speed Constraints, International Conference and Exhibition on Power Electronics and Motion Control- EPE-PEMC' 2010 Ohrid Macedonia.
[15] Vašak M., Baotić M., Petrović I., Perić N., Hybrid Theory-Based Time-Optimal Control of an Electronic Throttle, IEEE Trans. on Industrial Electronics, pp. 1483-1494, vol. 43, no.3 , 2007.
[16] Orłowska-Kowalska T., Bezczujnikowe układy napedowe z silnikami indukcyjnymi Oficyna Wydaw. PWr, Wrocław, 2003.
[17] Valenzuela M.A., Bentley J.M., Lorenz R.D., Evaluation of Torsional Oscillations in Paper Machine Sections, IEEE Trans. on Industry Applications, vol. 41, no.2 , pp. 493-501, 2005.
[18] Wang J., Zhang Y., Xu L., Jing Y., Zhang S., Torsional vibration suppression of rolling mill with constrained model predictive control, 6th World Congress on Intelligent Control and Automation, 2006, pp. 6401-6405, China.
[19] Maciejowski J.M., Predictive Control with Constraints, Prentice Hall, UK, 2002.
[20] Cychowski M.T., Robust Model Predictive Control, VDM Verlag, 2009.
[21] Kvasnica M., Grieder P., Baotic M., Morari M., Multi-Parametric Toolbox (MPT), HSCC (Hybrid Systems: Computation and Control), Lecture Notes in Computer Science, vol. 2993, 2004, pp. 448-46.
[22] Tøndel P., Johansen T.A., Bemporad A., An algorithm for multi-parametric quadratic programming and explicit MPC solutions, Automatica, 2003, 39, (3), pp. 489-497.
[23] Spjøtvold J., Kerrigan E.C., Jones C.N., Tøndel P., Johansen T.A., On the facet-to-facet property of solutions to convex parametric quadratic programs, Automatica, 2006, 42, (12), pp. 2209-2214.
[24] Bemporad A., Morari M., Dua V., Pistikopoulos E. N., The explicit linear quadratic regulator for constrained systems, Automatica, vol. 38, no. 1, pp. 3–20, Jan. 2002.

Acknowledgment

This research work is supported in part by the Ministry of Science and Higher Education (Poland) under Grant N N510 352936 (2009-2011).